Applied Physics A (2018) 124:172
https://doi.org/10.1007/s00339-018-1589-2

Applied Physics A
Materials Science & Processing

Birefringence profile adjustment by spatial overlap of nanogratings induced by ultra-short laser pulses inside fused silica

Atoosa Sadat Arabanian[1] · Somayeh Najafi[1] · Aliasghar Ajami[2] · Wolfgang Husinsky[3] · Reza Massudi[1]

Received: 25 November 2017 / Accepted: 15 January 2018

Abstract
We have succeeded in realizing a method to control the spatial distribution of optical retardation as a result of nanogratings in bulk-fused silica induced by ultrashort laser pulses. A colorimetry-based retardation measurement (CBRM) based on the Michel-Levy interference color chart using a polarization microscope is used to determine the profiles of the optical retardation. Effects of the spatial overlap of written regions as well as the energy and polarization of the writing pulses on the induced retardations are studied. It has been found that the spatial overlap of lines written by pulse trains with different energies and polarizations can result in an adjustment of the induced birefringence in the overlap region. This approach offers the possibility of designing polarization-sensitive components with a desired birefringence profile.

1 Introduction

Self-assembled nanogratings formed by focused femtosecond laser pulse trains inside a transparent media have opened new frontiers in micromachining ranging from 5D optical data storage [1], 3D integrated microfluidic sensors [2], nano-fluidics channels for lab on a chips [3, 4], to polarization-sensitive devices for optical circuits [5], such as polarization selective holograms [6], zero-order quarter-wave and half-wave retarders, and polarization beam splitters [7, 8].

When a sample is illuminated by several hundreds of ultrashort laser pulses, at certain intensity level, self-organized sub-wavelength periodic nanostructures oriented perpendicular to polarization of the writing beam can be generated in the focal region of the laser beam. The observed uniaxial birefringence due to such nanograting is called self-assembled form birefringence. Different techniques have been exploited to study such nanostructures, e.g. scanning electron microscope (SEM) [9–11], small angle X-ray scattering [9–11], and focused ion beam (FIB) milling [12]. Furthermore, various models have been proposed to explain the origin of these nanostructures. Shimotsuma et al., interpreted self-organized structures in terms of the interference of electron plasma waves resulting in electron concentration modulation, followed by freezing of the interference pattern by structural change in glass [13]. Beresna et al. [14] proposed that interference and dipole–dipole interaction of polaritons causes formation of nanogratings inside dielectrics. Also, surface plasma waves excited at the interface between the regions affected and unaffected by the femtosecond laser irradiation were introduced as trigger for the formation of nanogratings [15]. More recently, Rudenko et al. [16] proposed a numerical model based on Maxwell's equations coupled with multiple free carrier density rate equations and found that laser-induced inhomogeneities play a crucial role in generation of nanograting induced by femtosecond laser pulses. Moreover, the dynamics of the nanograting formation and the growth of nanograting-induced retardation has been experimentally studied by writing a series of dots inside fused silica using orthogonally polarized double pulses with different time delays [13, 17]. Generally, most reports are focused on the origin of nanogratings and the amount of retardation induced inside the material and, according to our knowledge, the spatial profile of the retardation in the modified region has not been considered yet.

In this paper, the spatial profile of the retardation induced by the nanogratings along the lines written by femtosecond

✉ Reza Massudi
r-massudi@sbu.ac.ir

[1] Laser and Plasma Research Institute, Shahid Beheshti University, G.c., Evin, Tehran, Iran

[2] Faculty of Physics, Semnan University, Semnan 35131-19111, Iran

[3] Institute of Applied Physics, Vienna University of Technology, Wiedner Hauptstrasse. 8 1060 Vienna, Austria

Published online: 24 January 2018

laser pulses is experimentally investigated. It is found that the amount of retardation varies from a maximum at the center to a minimum at the edges of the lines. We used a colorimetry-based retardation measurement (CBRM) method based on the Michel-Levy interference color chart using a polarization microscope to record 2D profiles of the retardation of lines. Effects of the lateral overlap of two adjacent lines created by a single pulse train as well as by an orthogonally polarized double pulse train on the optical retardation distribution have been studied. It is observed that by adjusting the polarization and the energy of the writing pulse trains as well as the line separation one can adjust the optical retardation in the overlap region of the lines. Such results offer the possibility of controlling the retardation induced by nanogratings to design polarization-sensitive components with a desired birefringence profile.

2 Experimental setup

The experiments have been performed with a mode-locked amplified Ti:Sapphire laser system (Femtolasers GmbH, FemtoPower Compact Pro.) operating at a wavelength of 800 nm with a pulse duration of 25 fs and a repetition rate of 1 kHz. It is possible to stretch the pulses up to 500 fs by adjusting the prism-pair position in the compressor part of the amplifier. The schematic of our experimental setup is illustrated in Fig. 1. The p-polarized laser beam enters a Mach–Zehnder interferometer and is equally divided by a non-polarizing 50/50 beam splitter. In the first arm, the pulse polarization changes to "s" using a half-wave plate to become orthogonal to that of the other arm. The two orthogonally polarized beams are recombined with a polarizing beam splitter. The optical path difference between two arms is adjusted so that the length of both arms are approximately equal. This is accomplished using an optical delay line in the first arm, with an accuracy better than the spatial length of the pulse, by observing the interference fringe pattern resulting from the second harmonic beam generated by a BBO crystal. The intensity ratio of the orthogonally polarized beams is varied by a half-wave plate inserted in the delayed path. To write lines inside a fused silica plate, the beam is focused using a microscope objective (Zeiss; 50 ×, 0.65 NA) at a depth of about 100 μm and is scanned inside the sample at a speed of 1 μm/s using a three-axis translation stage (ABL1050, Aerotech Ltd).

A positive optical phase-contrast microscope (PCM, Olympus BX50, 100 × oil-immersion objective) and a polarization microscope (Nikon, Optiphot2-pol, and 100 × oil-immersion objective) is used to image the distributions of the induced refractive index changes and the optical retardation of the lines, respectively.

3 Results and discussions

First, two parallel lines with a separation varying from 2 to 6 microns were written at a depth of 100 μm underneath the fused silica sample surface. Each line was written using a p-polarized femtosecond pulse train with a pulse duration of 100 fs and a pulse energy of 1 μJ. The lines were written with the same scanning direction to avoid the non-reciprocal "quill" effects that is described by Song et al. [18]. The spatial distributions of the refractive index change and the optical retardation of the two adjacent lines were verified using a PCM microscope (Fig. 2a1–c1) and the CBRM method using a polarization microscope (Fig. 2 a2–c2), respectively. The CBRM method is explained in "Appendix".

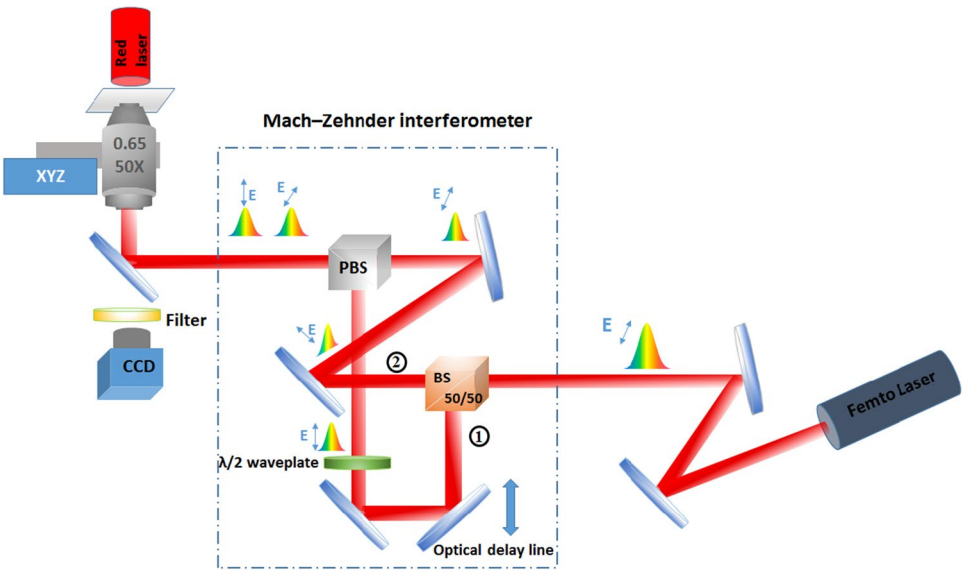

Fig. 1 Layout of experimental setup for generation of orthogonally polarized double pulse train and the femtosecond laser writing

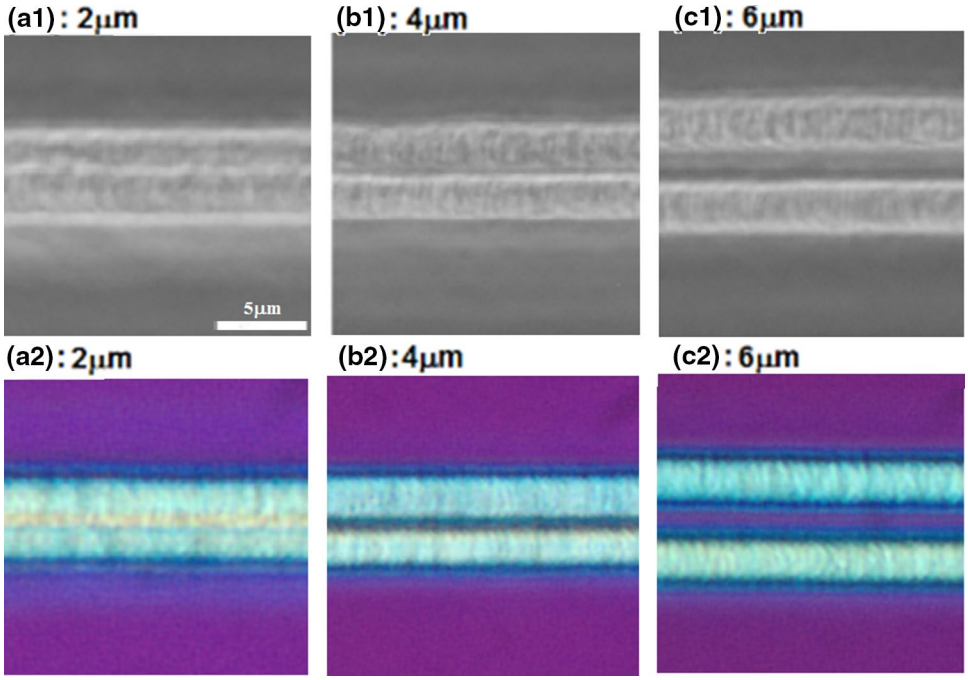

Fig. 2 the PCM images (**a1**–**c1**) and the CBRM images (**a2**–**c2**) of two lines with different separations between 2 and 6 μm

As known, the observed birefringence of each line is due to the induced nanograting structures and the direction of the slow axis of the uniaxial birefringence is always perpendicular to the polarization of the writing beam. Looking at a modified sample by a polarization microscope, the retardations arising from the sample and the tint plate are added/ subtracted, if the slow axis of birefringent lines are oriented parallel/perpendicular to the slow axis of the tint plate of microscope. Consequently, the observed interference color moves toward higher/lower order side of the Michel-Levy chart as compared to the purple background of the unmodified glass. For example, the blue-green color of the central part of each line, observed in the CBRM images of Fig. 2a2–c2, indicates that the directions of the slow axes of both lines are identical and perpendicular to the written lines. Therefore, the observed color of each line may illustrate the directions of the slow and the fast axes of the birefringent lines and, hence, the nanograting orientation.

Figure 2(c2) also shows that the blue-green color at the central part turns to the dark blue color at the edge of each line. It means that the retardation at the central part of each line is larger than at the edges. Comparing Fig. 2a2–c2 indicates that a decreasing line separation leads to an increase of the optical retardation in the overlap area, so that for a separation of 2 microns in Fig. 2a2, the overlap of the central parts of the two lines causes the yellow color for these regions in the CBRM image. According to the Michel-Levy chart, the yellow color indicates a larger optical retardation as compared to the blue-green color of the central part of each separate line.

To measure the amount of retardation in the overlap area for a line separation of 2 μm, the tint plate is replaced by a Senarmont compensator (see appendix). Figure 3a shows a microscopy image of lines when the analyzer axis is perpendicular to the polarizer axis of the microscope (i.e. the analyzer angle is set to zero degree). Turning the analyzer by an angle of 82°, the central part of each line turns to dark, which corresponds to an optical retardation of about 250 nm (Fig. 3b). However, the complete darkness of the overlap region occurs at an angle of 92° which corresponds to a retardation of about 280 nm (Fig. 3c). Variation of the optical retardation in the direction perpendicular to the modified lines observed in Fig. 3d confirms that the optical retardation in the overlap region of two lines with the same directions of birefringence axes is increased. We have also found that for a line separation larger than 6 μm the optical retardation of each line does not affect the other line and their extinction angle is about 70° (equivalent to retardation of 212 nm).

In the following experiments, we have studied the spatial distribution of an induced retardation when one line has been written by a pulse train with s-polarization and the other line with p-polarization and the two lines are laterally separated by 2 μm. The energies and the pulse durations of p- and s-polarized pulse trains are identical to the ones used in Fig. 2. The CBRM image of the induced retardation is shown in Fig. 4a and the inset of the figure illustrates the profile of retardation extracted from this image.

According to the Michel-Levy chart, an orange/blue color corresponds to a smaller/larger retardation as compared to the purple color of the background. Furthermore, it indicates that the slow axis of the line is parallel/perpendicular to the

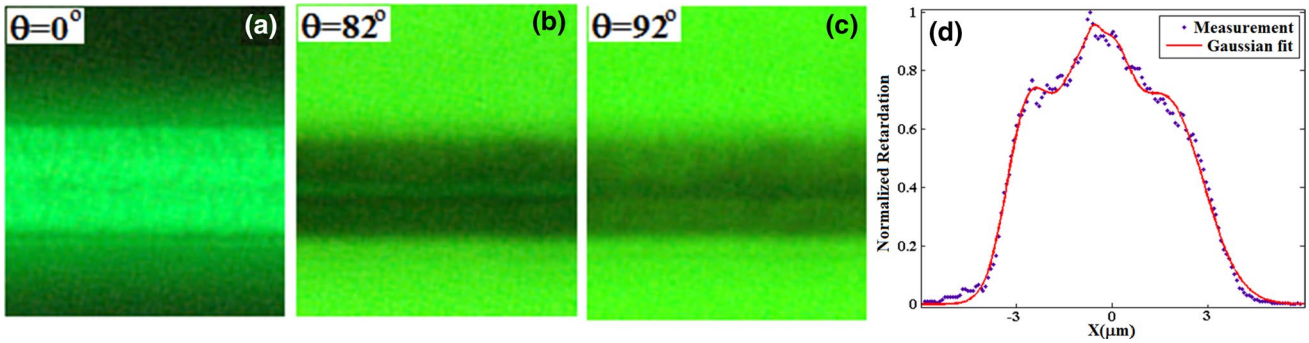

Fig. 3 The images acquired by using Senarmont measurements for analyzer rotation angle of **a** 0°, **b** 82° and 9 **c** 92° for lines separation of 2 μm, **d** variation of optical retardation in direction transverse to modified line structure

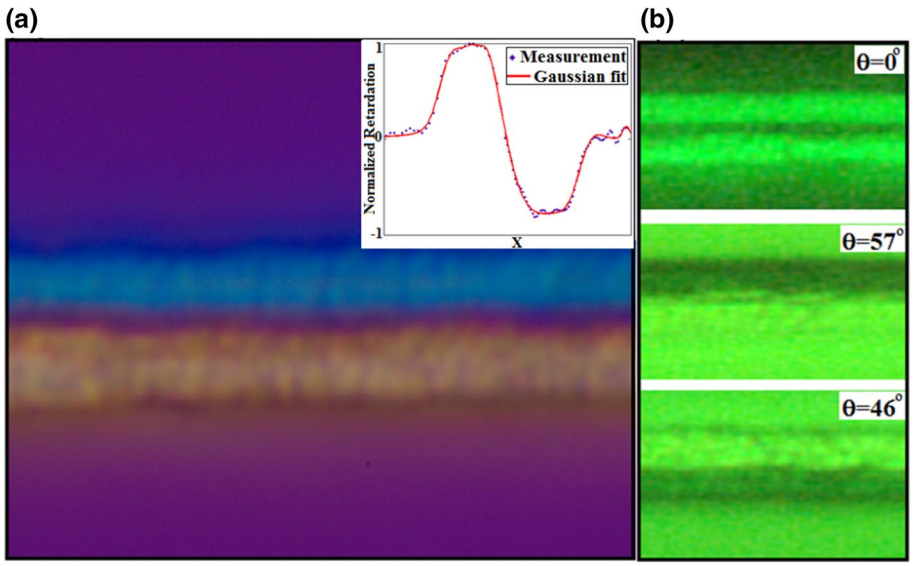

Fig. 4 **a** CBRM images of two lines inscribed by s-polarized and p-polarized pulse trains with pulse energy of 1μJ with transverse separation of 2μ m (inset: transverse profile of optical retardation). **b** The Senarmont images at different rotation angles of the analyzer

written line. This image illustrates that the retardation at the overlap region of two lines is almost canceled out due to their opposite signs. The cancellation of retardation is also confirmed by the dark color in the overlap region for an analyzer angle of zero when using the Senarmont method (Fig. 4b). This method gives the amount of retardation of the lines equal to − 140/173 nm (at analyzer angles of − 46/57° in Fig. 4b).

We also investigated the effect of a spatial overlap of regions modified by two orthogonally polarized simultaneous pulse trains with an energy of 0.5 μJ per pulse. To create such pulses, the p-polarized beam in the second arm of Mach–Zehnder interferometer in Fig. 1 is slightly tilted relative to the s-polarized beam in the first arm, so that only in a defined part of the modified region these beams spatially overlap. In the CBRM image (Fig. 5a), the color of the resulting modified region, which is a signature of the nanograting orientation, is determined by the relative intensity of the writing beams in the overlap region. Since the tilted p-polarized beam is not properly focused by the objective lens, it has a lower intensity relative to the focused s-polarized beam in the overlap region. Thus, the nanograting orientation in this region is determined by the s-polarized beam due to its higher intensity and mostly seen as orange color in Fig. 5a. However, on the edges of the line, where the beams do not overlap, the nanogratings are only created by the p-polarized beam (the blue edge). The purple color in the region marked as 'A' illustrates the nanogratings created by the orthogonal polarizations cancel each other.

Figure 5b shows a CBRM image acquired from two parallel lines separated by lateral distance of 2 microns, each one written by p-and s-polarized double pulse trains under the same conditions as for Fig. 5a. The CBRM image (Fig. 5b) and the Senarmont image with analyzer angle of zero degree (Fig. 5c, $\theta = 0$) show that the overlap region of the two lines, the region marked as "C", have the same color as the background which is due to cancelation of the optical retardation in those regions. Lateral variations of the

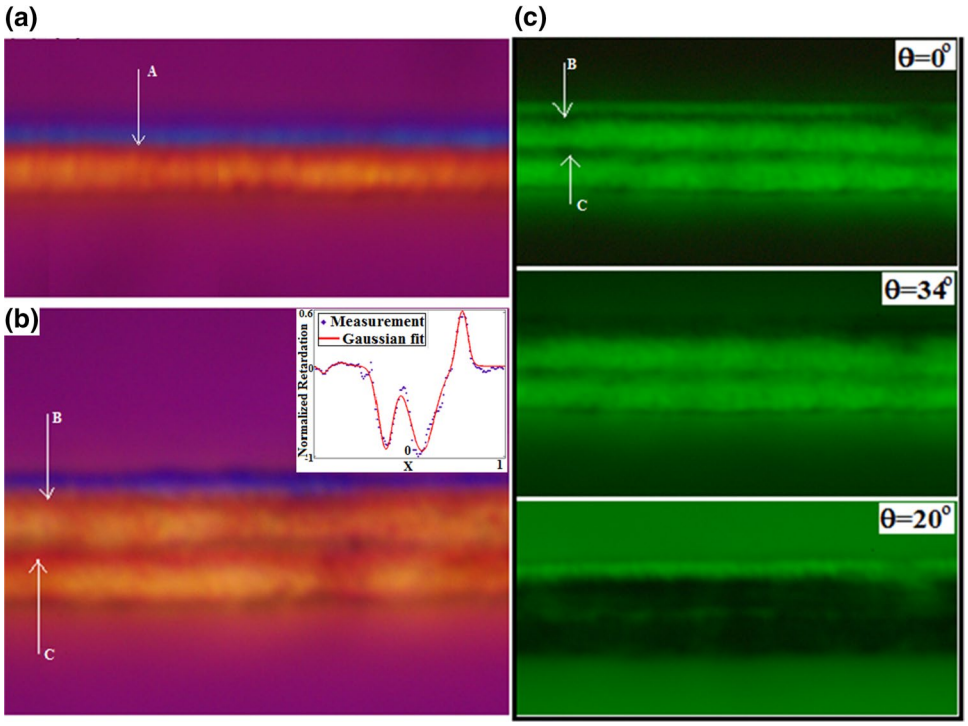

Fig. 5 **a** The CBRM image of a line written by orthogonally polarized double-pulse trains with p-polarized beam slightly tilted relative to s-polarized beam, **b** the CBRM image of two adjacent lines similar to line at **a** with a separation of 2 microns (profile of optical retardation is shown in the inset), **c** the Senarmont images with analyzer angles of 0°, − 34°, 20°, for two lines. The pulse energy for each pulse is 0.5 μJ

optical retardation perpendicular to the modified lines (inset of Fig. 5b) illustrates that the retardation is nearly zero in the regions marked as "B" and "C". Cancellation in "C" region is due to the spatial overlap of the nanostructures created by p-polarized pulses in the bottom line and those created by double pulses in the top line. The amount of optical retardation of the regions written by orthogonally polarized double pulses is about − 103 nm ($\theta = -34°$) while it is equal to 60 nm ($\theta = 20°$) for the birefringent region (the blue edge) induced by only p-polarized pulses (Fig. 5c). These results illustrate that by an appropriate adjustment of the lateral distance of two orthogonally polarized double pulse trains one can design a desired birefringence profile.

4 Conclusion

We have experimentally studied the influence of a spatial overlap of modified region written by ultrashort pulse trains with different polarizations and energies on the spatial distribution of the optical retardation induced by nanogratings. The CBRM method based on the Michel-Levy interference color chart was used to obtain retardation profiles and directions of the slow and the fast axes of the birefringent lines and, hence, the nanograting orientation. Our results demonstrate that the optical retardation of the spatially overlapped regions written by pulses with same polarization is enhanced while that of pulses with orthogonal polarizations is reduced. On the other hand, investigation of the spatial overlap of modified regions by two orthogonally polarized simultaneous pulse trains reveals that the nanograting orientation in each region is determined by the writing pulse with higher intensity. Therefore, the retardation at each point of the modified region can be controlled by adjusting the energy, polarization, and spatial overlap of the writing pulse trains. Such results can be attractive for the design of polarization-sensitive as well as polarization independent components.

Appendix

Colorimetry-based retardation measurement (CBRM) method [20] can be exploited using a polarization microscope to determine the induced optical retardation. In the CBRM method, a polarized white light enters into the sample that is placed between two cross-polarizers of the microscope so that its birefringence axes relative to polarizer and analyzer axes are 45°. Ordinary and extraordinary rays experience various phase difference passing through the sample, depending on the wavelength, that leads to different rotations of polarization for each wavelength of the white light. Superposition of transmitted waves with different wavelengths and amplitudes through the analyzer results in a color pattern where each color corresponds to a certain optical retardation experienced by the refracted ray. By comparing the observed colors with those contained on the Michel-Levy interference chart (Fig. 6), the retardations of each segment of the

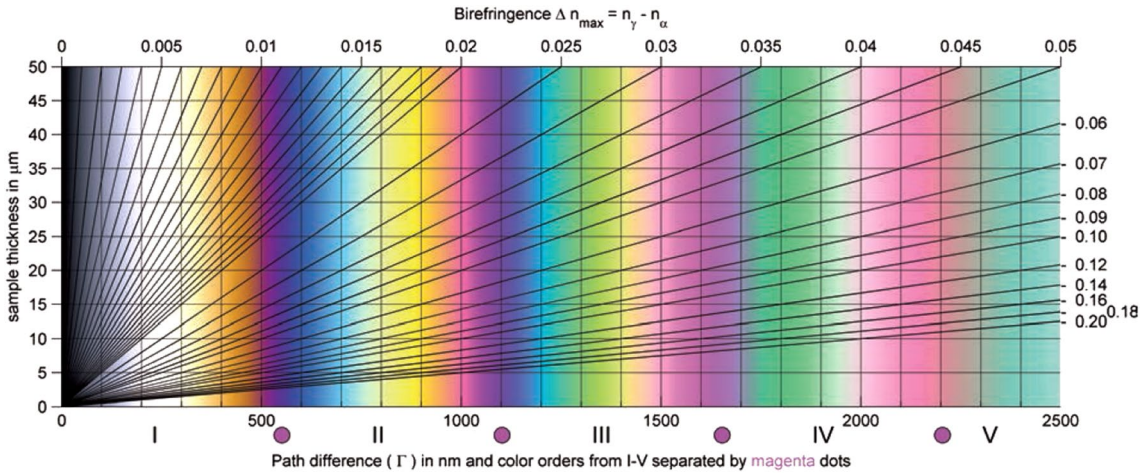

Fig. 6 Michel-Levy interference color chart [19]

modified structure of the sample can be estimated. To accurately determine small retardation values, a full-wave plate at $\lambda = 530$ nm (known as tint plate) should be inserted prior to the analyzer so that the measured retardation rises by one full wave of 530 nm. It is particularly useful for determining those retardations in the low first-order gray region of Michel-Levy chart (< 300 nm) that are the most difficult to estimate accurately.

The amount of the retardation for each segment can be measured by inserting a quarter-wave plate (known as Senarmont compensator) prior to the analyzer, instead of tint plate, and a narrowband green filter after the light source of the polarization microscope. By rotating of the analyzer by θ until where the birefringent region is darkened, the retardation (in nanometer) will be determined ($R = \lambda\theta/180$).

References

1. J. Zhang, M. Gecevičius, M. Beresna, P.G. Kazansky, in *CLEO: science and innovations, Optical Society of America*, CTh5D. 9 (2013). https://doi.org/10.1364/CLEO_SI.2013.CTh5D.9
2. Y. Hanada, K. Sugioka, I. Shihira-Ishikawa, H. Kawano, A. Miyawaki, K. Midorikawa, Lab Chip. **11**(12), 2109–2115 (2011)
3. Y. Liao, Y. Cheng, C. Liu, J. Song, F. He, Y. Shen, D. Chen, Z. Xu, Z. Fan, X. Wei, Lab Chip. **13**(8), 1626–1631 (2013)
4. Y. Cheng, Y. Liao, K. Sugioka, in *SPIE LASE*, p. 896708 (2014). https://doi.org/10.1117/12.2042742
5. W. Cai, A.R. Libertun, R. Piestun, Opt. Express **14**(9), 3785–3791 (2006)
6. L.A. Fernandes, J.R. Grenier, P.R. Herman, J.S. Aitchison, P.V. Marques, in *SPIE LASE, International society for optics and photonics*, p. 82470M (2012). https://doi.org/10.1117/12.2044740
7. A.R. Libertun, W. Cai, T. Gerke, R. Piestun, in *Photonic metamaterials: from random to periodic, Optical Society of America*, ThD18 (2006). https://doi.org/10.1364/OE.14.003785
8. M. Beresna, M. Gecevičius, P.G. Kazansky, Opt. Mater. Express **1**(4), 783–795 (2011)
9. S. Richter, A. Plech, M. Steinert, M. Heinrich, S. Doering, F. Zimmermann, U. Peschel, E.B. Kley, A. Tünnermann, S. Nolte, Laser Photonics Rev. **6**(6), 787–792 (2012)
10. S. Richter, C. Miese, S. Döring, F. Zimmermann, M.J. Withford, A. Tünnermann, S. Nolte, Opt. Mater. Express **3**(8), 1161–1166 (2013)
11. F. Zimmermann, A. Plech, S. Richter, A. Tünnermann, S. Nolte, in *SPIE LASE, International Society for Optics and Photonics*, pp. 935512–935516 (2015). https://doi.org/10.1002/lpor.201200048
12. S. Richter, S. Döring, F. Burmeister, F. Zimmermann, A. Tünnermann, S. Nolte, Optics Express **21**(13), 15452–15463 (2013)
13. Y. Shimotsuma, M. Sakakura, P.G. Kazansky, M. Beresna, J. Qiu, K. Miura, K. Hirao, Adv. Mater. **22**(36), 4039–4043 (2010)
14. M. Beresna, M. Gecevičius, P.G. Kazansky, T. Taylor, A.V. Kavokin, Appl. Phys. Lett. **101**(5), 053120 (2012)
15. Y. Liao, J. Ni, L. Qiao, M. Huang, Y. Bellouard, K. Sugioka, Y. Cheng, Optica. **2**(4), 329–334 (2015)
16. A. Rudenko, J.-P. Colombier, T.E. Itina, Phys. Rev. B. **93**(7), 075427 (2016)
17. Y. Shimotsuma, T. Asai, M. Sakakura, K. Miura, J. Laser Micro Nanoeng. **9**(1), 31 (2014)
18. H. Song, Y. Dai, J. Song, H. Ma, X. Yan, G. Ma, Appl. Phys. A. **123**(4), 255 (2017)
19. B.E. Sørensen, Eur. J. Mineral. **25**(1), 5–10 (2013)
20. C.C. Montarou, T.K. Gaylord, R.A. Villalaz, E.N. Glytsis, Appl. Opt. **41**(25), 5290–5297 (2002)